Institute of Physics Publishing Journal of Physics: Conference Series **50** (2006) 192–200
doi:10.1088/1742-6596/50/1/022 5th International Conference on Physics and Astrophysics of Quark Gluon Plasma

Recent Results on Strangeness and Heavy Flavour at RHIC

M A C Lamont†for the STAR Collaboration

† Physics Department, Yale University, New Haven, CT 06520, USA

E-mail: Matthew.Lamont@Yale.edu

Abstract.

The advent of RHIC has opened up the possibilities for a greater understanding of the hadronization process in relativistic heavy ion collisions. The large volume of data collected, together with high collisions energies, allows us to address both strangeness and charm production in great detail. This paper will present results on bulk strangeness production in Au+Au collisions at $\sqrt{s_{NN}}$ = 200 GeV, in particular on strangeness enhancement and strange quark scaling. Also presented are results on strange particle ratios and elliptic flow measurements in the intermediate p_T region, together with comparisons with theoretical models. An excitation function of strangeness yields and ratios are also presented with reference to the newly acquired Au+Au data at $\sqrt{s_{NN}}$ = 62.4 GeV.

Also presented in this paper are the first results on charm production measured in STAR. Utilising the methods of reconstructing D mesons through their leptonic channels, the cross-section for charm production in d+Au collisions at $\sqrt{s_{NN}}$ = 200 GeV is presented. Also shown is a first measurement of the elliptic flow of charmed mesons.

1. Strangeness Production at RHIC

1.1. Strangeness enhancement

The enhancement of strange particles in A+A collisions, with respect to p+p collisions, has long been predicted as a signature of a de-confined state of matter [1]. When calculating expected values for this enhancement, care has to be taken with the differences in the size of the system. This is achieved by utilising a canonical partition function for the smaller systems, where relevant quantum numbers must be conserved explicitly. For the larger volume A+A collisions though, a grand canonical partition function may be used which allows for the conservation of quantum numbers on the average. Utilising these models, predictions for strangeness enhancement as a function of strangeness, centrality and centre of mass energy have been obtained [2]. It is expected that the enhancement factors increase with strangeness content and centrality and are greatest at the lower SPS energies.

The $<p_T>$ of strange baryons in A+A collisions is approximately 1.1 GeV/c and hence the production of strange particles is predominantly in the p_T region below 2 GeV/c. Therefore, when comparisons are made between different collision systems regarding strangeness enhancement, it is typically this low p_T region which is being measured. STAR has good capabilities in measuring strange hadrons via their decay topology in the TPC in this p_T range, with acceptance down to a few hundred MeV [3]. Good coverage at low p_T is important as it

allows for the constraint of fits, used to determine the yields ($dN/d\mathbf{y}$), as the data turns over at low p_T in A+A collisions (when plotted versus $m_T - m_0$) due to transverse radial flow.

The dependence of strangeness enhancement has been studied at the SPS in some detail for a number of lower energies than RHIC is capable of. Data on strangeness enhancement in Pb+Pb collisions are shown in the left two panels of Figure 1 [4]. While these data exhibit the expected ordering with respect to strangeness content of the hyperon, there appears to be no dependence on beam energy for both hyperons and anti-hyperons. The enhancement factors for the $\Lambda(\overline{\Lambda})$ and $\Xi^-(\overline{\Xi}^+)$ have also been calculated for Au+Au collisions at 200 GeV in STAR and is shown in the right panel of Figure 1. Note that there is no data from the $(\Omega^- + \overline{\Omega}^+)$ in the STAR figure. This comes from the lack of p+p reference data at 200 GeV on $(\Omega^- + \overline{\Omega}^+)$ production.

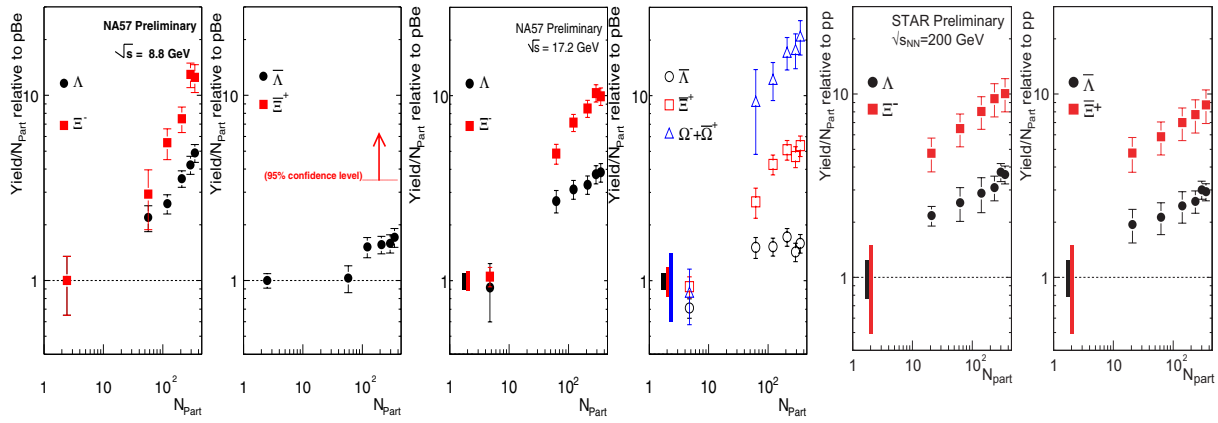

Figure 1. The enhancement factors for hyperons and anti-hyperons as a function of centrality for data from Pb+Pb collisions at $\sqrt{s_{NN}} = 8.8$ GeV (left panel), Pb+Pb collisions at $\sqrt{s_{NN}} = 17.2$ GeV (centre panel) and Au+Au collisions at $\sqrt{s_{NN}} = 8.8$ GeV (right panel).

It is evident that the predicted energy dependence of strangeness enhancement is not observed in the data. Although there is a dependence on energy of the strangeness yields in A+A collisions, the enhancement factors are affected by the increase in available energy for production in the reference systems. One other point of note from Figure 1 is that at the lower energies, the enhancement of the $\overline{\Lambda}$ appears to be constant with centrality (defined by the number of participants in the collision, N_{part}), whereas at the higher energy, no saturation is observed.

This observation initiated work on the fact that the volume may not scale linearly with N_{part}. It was found that when the valence quarks of a hadron were scaled with N_{part} for the light quarks and with the number of binary collisions (N_{bin}) for the strange quarks, then the yield of particles from peripheral to central A+A collisions appears to be constant [5].

1.2. Strangeness production at intermediate p_T

Also presented at this conference were results from the intermediate p_T region (defined in this paper as $2 < p_T < 6$ GeV/c). There has recently been a lot of interest in this range of the particle spectra, in particular for identified particles. This was initiated by results noting differences between $\overline{p}$ and π spectra measured by PHENIX [6]. PHENIX showed that in the most central dataset, the ratio of $\overline{p}/\pi$ increased with p_T up to 3 GeV/c where the statistics end. This is well above the ratio measured in elementary collisions [7]. In peripheral collisions, however, the situation is different and the ratio does follow that observed in elementary collisions.

One explanation of these phenomena is that the baryons and mesons are simply produced by the coalescence/recombination of thermal partons from the plasma. If that were the case,

then this intuitively leads to a rising baryon/meson ratio. Various coalescence models produced post-dictions for the baryon/meson ratio which agreed well with the $\overline{p}/\pi$ measurements from PHENIX. All models showed that the ratio peaks in this intermediate region, and actually starts to decrease after $p_T \approx 4$ GeV/c [8–10].

In order to test the models further, it was required to extend the particle identification to higher transverse momenta. Using Λ and K^0_S measured in STAR, it is possible to reproduce the baryon/meson ratio and extend the measurement to higher p_T as the upper limit in p_T of Λ and K^0_S reconstruction is only limited by statistics. In the 200 GeV Au+Au run in 2001, it was possible to measure the Λ and K^0_S out to 6 GeV/c in p_T in the most central data, and out to 4.5 GeV/c in the most peripheral centrality bin. The Λ/K^0_S ratio is illustrated in the left panel of Figure 2 as a function of centrality in Au+Au collisions, together with data from p+p collisions at $\sqrt{s} = 200$ GeV.

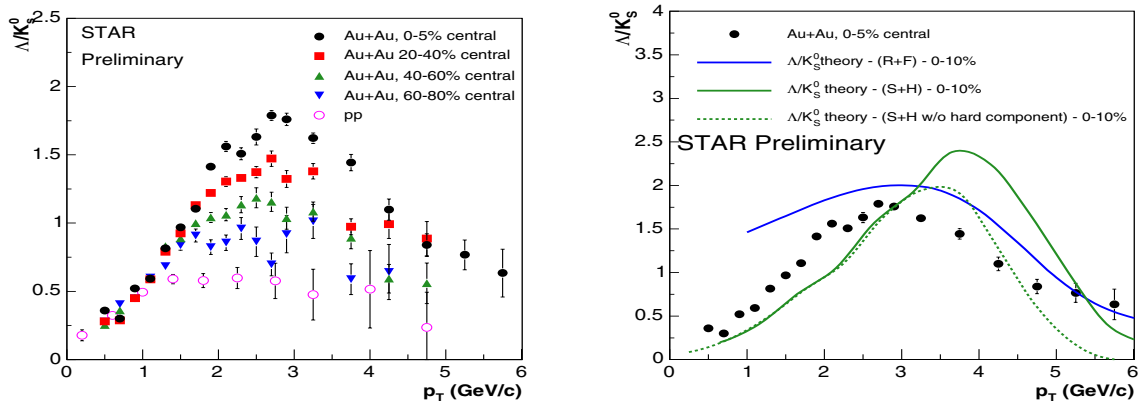

Figure 2. Left panel : The Λ/K^0_S ratios as a function of p_T and centrality for Au+Au and p+p collisions at $\sqrt{s_{NN}} = 200$ GeV. Right panel : The Λ/K^0_S ratio for the most central Au+Au bin together with theoretical predictions.

This data clearly exhibit a strong centrality and p_T dependence of the ratio. The ratio rises smoothly with increasing centrality, reaching a maximum at around $p_T \approx 3$ GeV/c before turning over and reducing towards the values obtained in the peripheral collisions. Due to the limited statistics with this dataset, it is not yet possible to determine at what value of p_T the ratio returns to the value from p+p collisions.

A comparison of this ratio to different coalescence models has been performed and is shown in the right panel of Figure 2. The first model (R+F) uses just recombination of thermal quarks and fragmentation at higher p_T [8] whereas the second model (S+H) allows the coalescence of soft and hard partons [9]. Though the models do not reproduce the data quantitatively, they do reproduce the qualitative details of the ratio well. One important prediction that is not yet available from these models is that of the centrality dependence of the ratios.

Another measurement using strange particles in the intermediate p_T region is that of the elliptic flow (v_2) of particles with respect to the reaction plane of the collision. This measurement is presented in the left panel of Figure 3 for Au+Au collisions at $\sqrt{s_{NN}} = 200$ GeV, averaged over all centralities. The results shown in the left panel of Figure 3 are important as they show that not only do the light particles flow, but the Ξ and Ω also flow with the same magnitude as the lighter hadrons. It has been shown previously that the Ξ and Ω have a smaller radial flow component than the lighter particles, which has been attributed to their presumably low hadronic cross-sections [11]. Though the v_2 is built up throughout the lifetime of the collision,

the greatest contribution to the v_2 comes when the nuclear volume is most asymmetric in the early stages. As both the Ω and Ξ exhibit elliptic flow of the same magnitude as the Λ and K^0_S, it appears that this may be partonic in origin. To extend this hypothesis further, the measured v_2 of the different particles is divided by the number of valence quarks and plotted against the p_T similarly scaled by the number of valence quarks in the right panel of Figure 3.

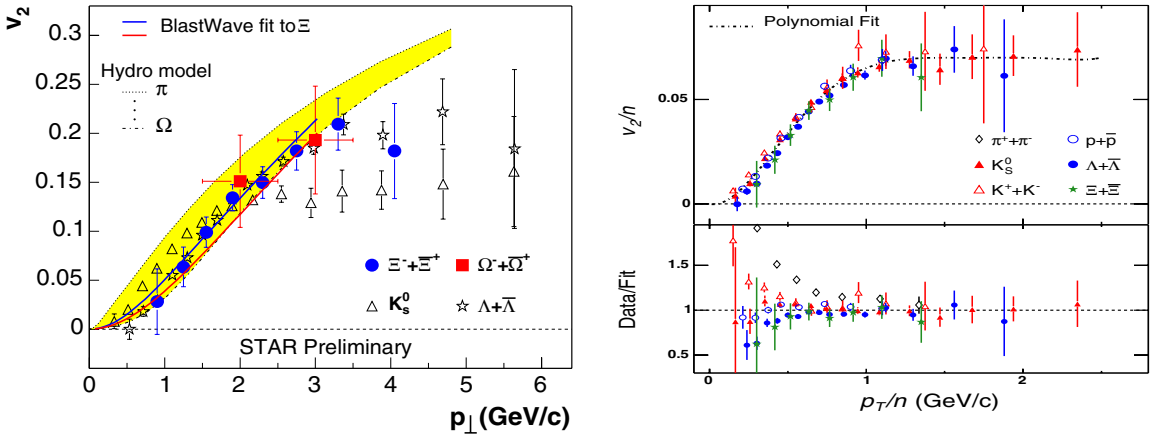

Figure 3. Left panel : The measured v_2 for strange particles at 200 GeV as a function of p_T plotted together with predictions from a hydrodynamical model and a blastwave fit to the pion v_2. Right panel : The elliptic flow at 200 GeV scaled by the number of valence quarks, plotted versus p_T scaled by the same number.

Together with the K^0_S, Λ and Ξ from STAR, data for pions, protons and charged kaons from PHENIX are also shown. The lower panel represents the deviation from a fit to the data. With the exception of the pions, the particles appear to scale well, with the largest deviations occurring at low p_T/n, in a region presumably dominated by hydrodynamics. This scaling is naturally reproduced in the coalescence models where the elliptic flow is built up when the collision is in the deconfined state.

Although there are a number of outstanding questions pertaining to the validity of the use of coalescence models, such as entropy conservation, the inclusion of higher Fock states (though this has been addressed recently [12]) and the use of a thermal mass for the constituent quarks of $\approx$ 300 MeV/c^2, it is clear that they can reproduce a number of features of the data. In all the different implementations, the coalescence mechanism dominates over fragmentation up to transverse momenta of about 6 GeV/c and it is therefore possible to divide the particle production into a number of different regimes : hydrodynamics, recombination, modified fragmentation and pure fragmentation.

Also shown at this conference were first results on strangeness production from Au+Au collisions at $\sqrt{s_{NN}}$ = 62.4 GeV. Excitation functions of both the yield and ratios of the singly and multiply strange particles showed little deviation from a common trend observed between the lower energy SPS data and the full energy RHIC data, mapping out the net baryon density dependence of the energy of the collision [13]. It was also found that the valence quark scaling of the v_2, as discussed earlier, also holds for the data at 62 GeV.

2. Heavy Flavour Production

2.1. Charm production cross section

The measurement of heavy quarks in relativistic heavy ion collisions is important as, due to their large masses, their production can be calculated in pQCD, even at low momenta. The calculation

of the charm production cross section at RHIC energies is important in order to map out the area between $\sqrt{s} \approx 60$ GeV and $\sqrt{s} \approx 900$ GeV where there are existing measurements [14].

The reconstruction of charm is different to the well established topological analysis used for strange particles described in the previous section. In STAR, there are two methods used to reconstruct D mesons which are explained below.

Due to their short lifetimes, direct reconstruction of the decay vertex is not possible. Therefore a technique which takes all kaons and pions, identified through their specific ionisation in the TPC, and calculates an invariant mass distribution is used. The background is estimated by performing the same calculation on kaons and pions from different events, a technique which removes all possible correlations. Though this technique allows direct identification of D mesons, the branching ratio into this channel is very small at ≈ 4 %. The left panel of Figure 4 shows a mass plot before and after background subtraction. One setback of this technique is that D^0s are only reconstructed in the low p_T region.

In order to extend the reconstruction of D mesons to higher p_T, they are measured via their semi-leptonic decay channels. Electrons are initially identified in the TPC through their specific ionisation in the momentum range of 1.5 to 8 GeV/c where their dE/dx is higher than that of hadrons. This technique provides an e/h discrimination power of approximately 500. At low momentum ($0.2 < p_T < 3$ GeV/c), electrons can be identified in the STAR Time of Flight system, combining the measured velocity with the dE/dx information from the TPC. A cut on $|1/\beta - 1| \leq 0.003$ eliminates the hadrons crossing the electron band at low momentum. At higher momenta, electron candidates which pass the dE/dx cuts are extrapolated to the Barrel Electro-magnetic Calorimeter (EMC). The p/E_{tower} (where E_{tower} is the energy of the tower) of the candidates is then calculated as shown in the right panel of Figure 4. The electrons, due to their low mass, show a peak at ≈ 1, given by the filled in region in the plot whilst hadrons have a much wider distribution. Energy leakage to neighbouring towers means that the peak is not centred at 1, but this is expected and understood using GEANT simulations.

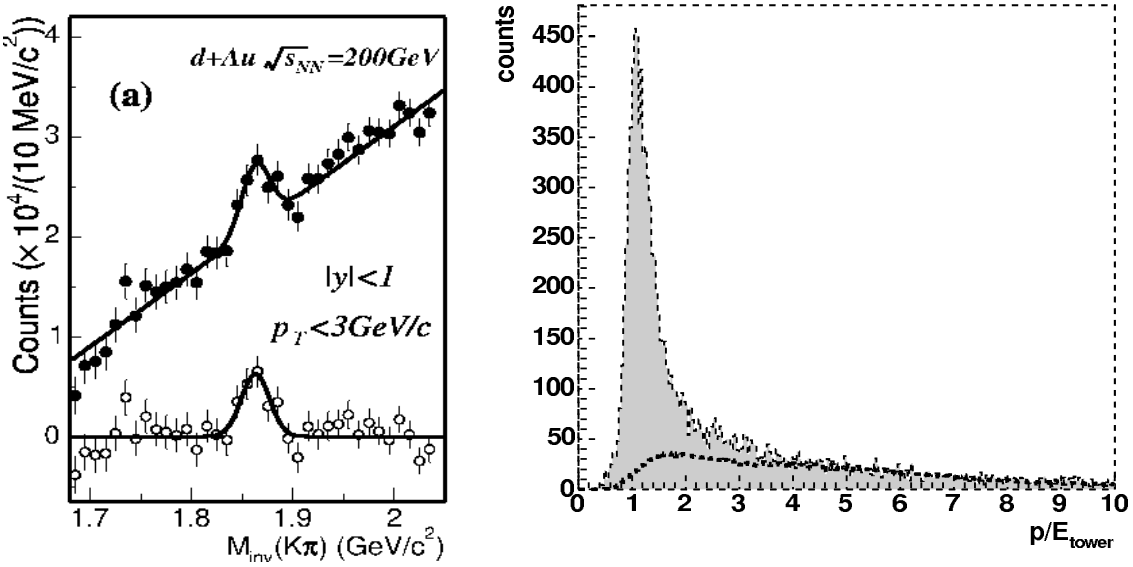

Figure 4. Left panel : Invariant mass distributions for the D^0 before and after background subtraction. Right panel : The measured p/E_{tower} for particles in the electro-magnetic calorimeter.

Another important detector is the Shower Max Detector (SMD) which provides for greater segmentation than the EMC alone. This enables the differentiation between electronic and

hadronic signals through their profile: electronic showers tend to be more developed compared to hadronic showers. Whereas the background to the direct reconstruction of D mesons through the hadronic channel mainly comes from combinatorial effects, the semi-leptonic channel also has background sources of electrons. The majority of the background comes from photonic sources, such as π^0 Dalitz decays and photon conversions in the detector material. These can be reduced by calculating the invariant mass of di-electron pairs, and removing those pairs whose $m^2_{inv} < 0.02$ (GeV/c^2)^2. Non-photonic sources, such as misidentified hadrons, leptons from heavy quarks and Drell-Yan, also contribute to the background but at a much smaller level and are estimated through simulation.

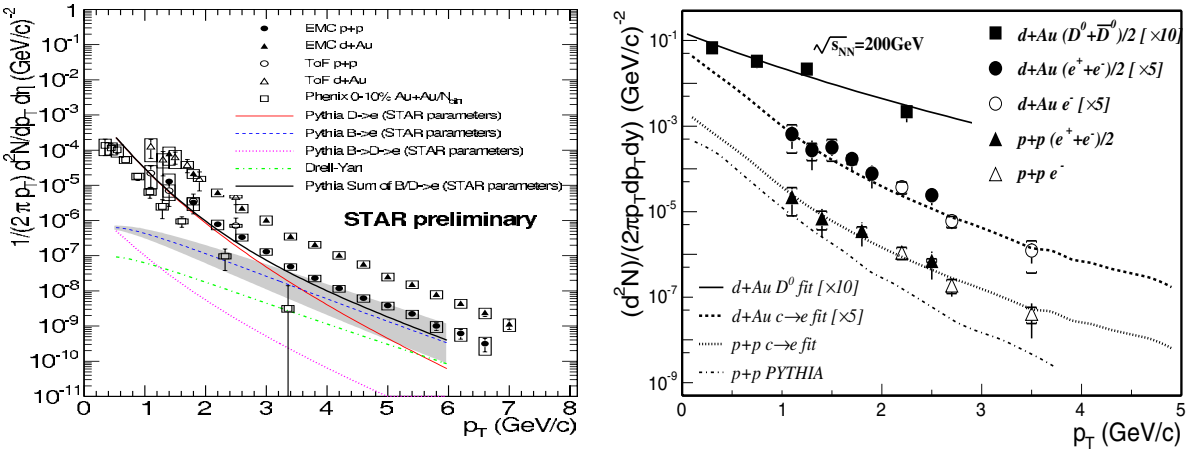

Figure 5. Left panel : STAR electron spectra from the Time Of Flight and Electro-magnetic Calorimeter detectors, together with contributions from a PYTHIA parameterisation. Right panel : Fits to the STAR electron and D^0 spectra.

The left panel in Figure 5 shows the electron spectra in both p+p and d+Au collisions over the full range in p_T using both the TOF and EMC detectors. Also shown are the various contributions to the spectrum from D and B decays, obtained by running Pythia with the parameters outlined elsewhere [15]. A simultaneous fit to the STAR electron data (from dE/dx and TOF only) together with the directly reconstructed D^{0}s was performed and is presented in the right panel of Figure 5.

The total cross section of charm production per nucleon-nucleon interaction in d+Au collisions from the combined fit is 1.4±0.2±0.4 mb which is in agreement with that obtained from fitting the D^0 spectra separately [16]. This is compared with other measurements as a function of energy in Figure 6, together with LO and NLO pQCD calculations. Although the STAR measurement appears to be high when compared to the PHENIX measurement and pQCD predictions, it is not inconsistent with measurements from cosmic ray experiments at $\sqrt{s} = 300$ GeV.

2.2. Charm flow

One of the highlights from the strangeness section of this paper is that the measured v_2 of the strange hadrons appears to scale well with the number of valence quarks, which in turn led to the proposal of a number of coalescence/recombination models. It was proposed that if RHIC is hot and dense enough to produce a deconfined medium in Au+Au collisions, then charm quarks may be thermalised [17]. If this is the case, then they may also exhibit finite elliptic flow.

In Au+Au collisions, it is not possible to reconstruct D^0 mesons explicitly due to the large combinatorial background. We therefore must rely upon the technique which reconstructs them through their semi-leptonic decay channel. One important question is whether the elliptic flow of the measured electrons is representative of the meson flow? This is answered via simulations

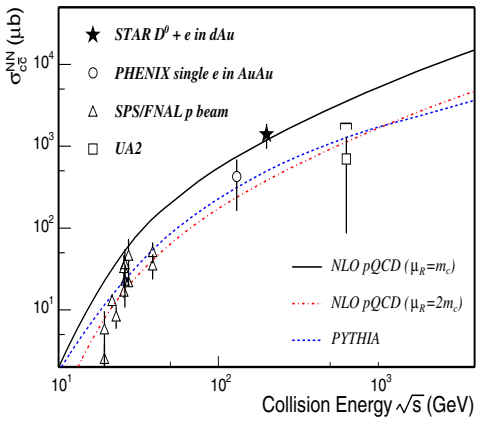

Figure 6. The measured charm production cross section as a function of energy.

and is shown in the left panel of Figure 7. It is evident that if the electron momentum is in the range 2 -3 GeV/c, there is a very strong corrrelation between the emission direction of the D meson and the decay direction of the resulting electron. Only data from the low momentum region is available due to the limited scale of the available calorimeter in the first Au+Au run at $\sqrt{s_{NN}} = 200$ GeV.

The data used in this analysis are the 80% most central Au+Au collisions, constituting approximately 2 M events from the 2001 data taking period. The same technique as described in the previous section was used to remove background from the data sample. The electrons which still pass the various cuts are estimated to be mainly from D-meson decays (63%), the remainder ((37%) are from γ conversions and π^0 Dalitz decays. The azimuthal angles of the remaining electrons are then correlated with the reaction plane angles and the $\cos(2[\phi\text{-}\psi_{RP}])$ distribution calculated, as described elsewhere [18].

The azimuthal distribution of the background is simulated and then scaled using the π^0 single particle spectrum obtained from PHENIX [19]. This distribution is then subtracted from the total electron spectrum and the v_2 of the remainder is the calculated. This is done as a function of p_T and the result is shown in the right panel of Figure 7, where the error bars are statistical only and do not include an estimated 25% systematic error.

Also shown are data at lower p_T from PHENIX [20] together with predictions from the MP parton cascade model for the v_2 for D mesons themselves, and also the electrons coming from D mesons [21]. There are two scenarios, one where the charm quark has no flow (but the light quarks do), and one where the charm quark has as much flow as the light quarks. Within this model, the measured v_2 of the electrons in this p_T range agrees with the prediction where the charm quark flows as the light quarks, though the large systematical errors, still under investigation, do not rule out the first scenario.

3. Summary

In summary, this paper presented results on strangeness and charm production at RHIC. It was shown that understanding the enhancement of strangeness is a complicated process and a full understanding of the production of strangeness in p+p collisions as a function of energy is still required. In the intermediate p_T region, it was shown that there is a very large difference between the production of strange baryons and mesons which is not reproduced in elementary particle collisions. However, it can be explained by models which invoke the coalescence/recombination of constituent quarks. This leads to a natural explanation of the baryon/meson ratio and the common v_2 dependence with p_T when scaling both variables by the number of valence quarks in

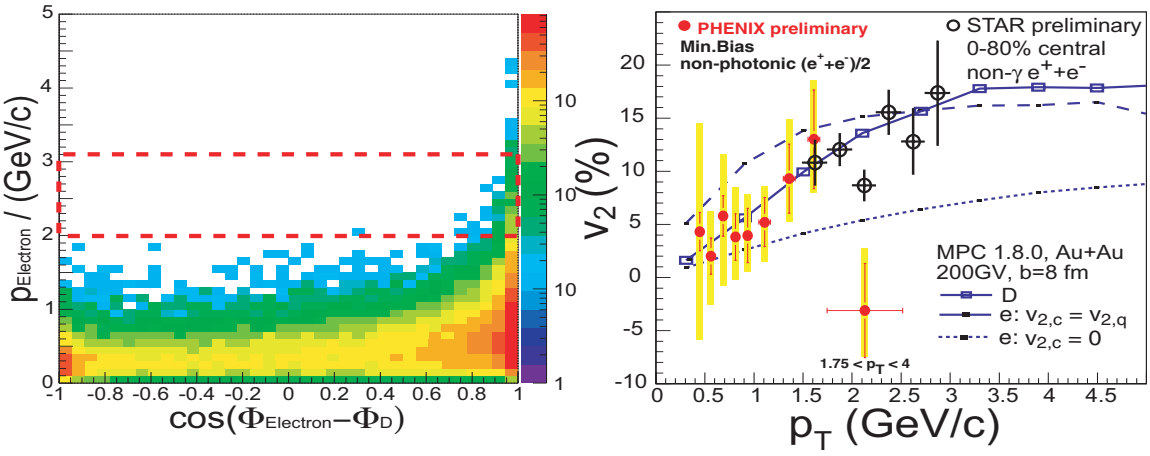

Figure 7. Left panel : The simulated relative angles in azimuth between the electron and the D meson. Right panel : The measured electron v_2 measured in STAR, together with preliminary data from PHENIX at lower p_T, and a theoretical model prediction.

the relevant hadron. The nucleon-nucleon production cross section of charm in d+Au collisions was also presented, obtained through both the hadronic and semi-leptonic decay channels. It was found to be slightly higher than model predictions though is in agreement with the trend of cosmic ray measurements at higher energies. A measurement of the elliptic flow (v_2) of electrons in STAR was presented, under the assumption that they originate from D mesons. The v_2 measurement extended the reach of an earlier PHENIX measurement. The data indicate that the charm quark flows as strongly as the light quarks when compared to a coalescence model, though the systematic errors on the measurement do not allow a definitive statement.

4. Acknowledgements

We thank the RHIC Operations Group and RCF at BNL, and the NERSC Center at LBNL for their support. This work was supported in part by the HENP Divisions of the Office of Science of the U.S. DOE; the U.S. NSF; the BMBF of Germany; IN2P3, RA, RPL, and EMN of France; EPSRC of the United Kingdom; FAPESP of Brazil; the Russian Ministry of Science and Technology; the Ministry of Education and the NNSFC of China; Grant Agency of the Czech Republic, FOM of the Netherlands, DAE, DST, and CSIR of the Government of India; Swiss NSF; the Polish State Committee for Scientific Research; and the STAA of Slovakia

5. References

[1] Rafelski J and Muller B 1982, *Phys. Rev. Lett.* **48** 1066
[2] Tounsi A, Mischke A and Redlich K, 2003, *Nucl. Phys.* A**715** 565
[3] Adler C *et al* (STAR Collaboration) 2002, *Phys. Rev. Lett.* **89** 092301
Adams J *et al* (STAR Collaboration) 2004, *Phys. Rev. Lett.* **92** 182301
[4] Elia D for the NA57 Collaboration 2005, *J. Phys. G: Nucl. Phys.* **31** S135
[5] Caines H (for the STAR Collaboration) 2004, *Preprint* nucl-ex/0412015
[6] Adcox K *et al* (PHENIX Collaboration) 2004, *Phys. Rev.* C **69** 024904
[7] Abreu P *et al* (DELPHI Collaboration) 2000, *Euro. Phys. J.* C **17** 207
[8] Fries R J, Muller B, Nonaka C, Bass S A 2003, *Phys. Rev.* C **68** 044902
[9] Greco V, Ko C M and Levai P 2003, *Phys. Rev.* C **68**, 034904
[10] Hwa R C and Yang C B 2003, *Phys. Rev.* C **67** 034902
[11] Adams J *et al* (STAR Collaboration) 2004, *Phys. Rev. Lett.* **92** 182301
[12] Fries R J, Muller B, Nonaka C, Bass S A 2005,*Preprint* nucl-th/0503003
[13] See proceedings of Strange Quark Matter 2004 to be published in *J. Phys. G: Nucl. Phys.*
[14] Rakobolskaya I N, Roganova T M and Sveshnikova L G 2003, *Nucl. Phys. B − ProceedingsSupplements* **122** 353

[15] Suaide A A P(for the STAR Collaboration) 2004, *J. Phys. G: Nucl. Phys.* **30** S1179
[16] Adams J *et al* (STAR Collaboration) 2005, *Phys. Rev. Lett.* **94** 062301
[17] Greco V, Ko C M and Rapp R 2004, *Phys. Lett.* B**595** 202
[18] Laue F (for the STAR Collaboration) 2005, *J. Phys. G: Nucl. Phys.* **31** S27
[19] Adler S S *et al* 2003, *Phys. Rev. Lett.* **91** 0702301
[20] Kaneta M *et al* 2004, *J. Phys. G: Nucl. Phys.* **30** S1217
[21] Molnar D 2005, *J. Phys. G: Nucl. Phys.* **31** S421